A new structural type for a binuclear chloride-bridged copper(II) complex. Structural and magnetic characterization of di-μ-chloro-chloropentakis(benzimidazole) dicopper(II) monochloride tetrahydrate, $[Cu_2Cl_3(C_7H_6N_2)_5]Cl \cdot 4H_2O$

A. Tosik, W. Maniukiewicz, M. Bukowska-Strzyzewska*
Institute of General Chemistry, Technical University of Lødz, Zwirki 36 (Poland)

J. Mrozinski*
Institute of Chemistry, University of Wrocław, 50 383 Wrocław (Poland)

M. P. Sigalas and C. A. Tsipis*
Laboratory of Applied Quantum Chemistry, Department of General and Inorganic Chemistry, Faculty of Chemistry, Aristotelian University of Thessaloniki, 54 006 Salonica (Greece)

(Received May 3, 1991; revised August 2, 1991)

Abstract

The synthesis, crystal structure determination and magnetic properties of a new five-coordinated unsymmetrical copper(II) dinuclear complex $[Cu_2Cl_3(C_7H_6N_2)_5]Cl \cdot 4H_2O$ are reported. The crystals are orthorhombic, space group *Pnma* with 4 formula units in a cell of dimensions: $a = 19.506(3)$, $b = 17.384(4)$, $c = 11.940(2)$ Å. The structure was solved by direct methods. Least-squares refinement using 2138 independent reflections with $I \geqslant 3\sigma(I)$ has led to a final value of the conventional R factor (on F) of 0.047 and R_w of 0.049. The complex cation consists of pairs of deformed trigonal-bipyramidal copper(II) centers which share an edge by two equatorial chloride ions. The equatorial coordination sites of the Cu(1) atom are occupied by three chloride ligands, while of the Cu(2) atom by two chloride and one benzimidazole ligands. The axial sites are occupied by the nitrogen atoms from four benzimidazole ligands. The Cu atoms and equatorial ligands are located on the symmetry plane. The Cu–Cu non-bonding distance in the complex is 3.386(1) Å; the two shorter bridging Cu(1)–Cl(1) and Cu(2)–Cl(1) distances are 2.402(2) and 2.424(2) Å; the two longer Cu(1)–Cl(2) and Cu(2)–Cl(2) are 2.620(2) and 2.551(2) Å. The Cu(1)–Cl(1)–Cu(2) and Cu(1)–Cl(2)–Cu(2) angles are 89.1(1) and 81.8(1)°. The structure is the first example of a bibridged binuclear complex with two non-equivalent Cu–Cl–Cu bridges. Comparison to other binuclear bis(μ-halide)-bridged copper complexes of similar structure has been made. Magnetic susceptibility measurements indicate ferromagnetic coupling of the copper(II) centers, the intramolecular exchange parameter, $2J$, being 5.6 cm^{-1} and the intermolecular one $J' = -0.6$ cm^{-1}. The investigation of the electronic structure of the complex and the orbital interpretation of the magnetic coupling based on extended Hückel molecular orbital calculations are also presented.

Introduction

Correlation between the exchange energy, $2J$, and the structure of the binuclear transition metal complexes has received considerable attention from many researchers. Most of these works have been concentrated on the copper(II) complexes since the d^9 configuration of Cu(II) ion involves only one magnetic orbital in the exchange process and the structural chemistry of copper(II) chlorides and bromides is extremely diverse as a result of that metal's flexible coordination geometry. Thus, the structures of a number of halogen-bridged copper(II) complexes have been investigated in hope of correlating their structural and magnetic properties [1–11] and Hodgson and co-workers [12] have proposed an empirical correlation between the exchange energy and the φ/R ratio (φ is the Cu–Cl–Cu bridging angle and R is the longer Cu–Cl distance in the bridge) in the case of bis-chloro-bridged copper(II) complexes with each copper center adopting a square-pyramidal or trigonal-bipyramidal geometry.

In this paper the synthesis, crystal structure and results of magnetic studies of a new five-coordinate

*Authors to whom correspondence should be addressed.

0020-1693/91/$3.50

unsymmetrical copper(II) binuclear complex with chloride and benzimidazole ligands are discussed, in comparison with other copper(II) complexes of similar structure. Moreover a study of the electronic structure and an interpretation of its magnetic behavior, based upon EHMO LCAO MO quantum-chemical calculations are also presented.

Experimental

Synthesis

The complex was prepared by adding a warm aqueous solution of the metal salt (1.7 g of $CuCl_2 \cdot 2H_2O$ (0.01 mol) in 25 ml of water with 0.5 ml of concentrated HCl) to a warm aqueous solution of benzimidazole (1.16 g (0.01 mol) in 25 ml of water). Slow evaporation deposited well formed pale-green crystals analysed as $Cu_2Cl_4 \cdot 5(C_7H_6N_2) \cdot 4H_2O$. *Anal.* Found: C, 45.16; N, 15.05; Cl, 15.27; H, 4.08. Calc. for $Cu_2Cl_4 \cdot 5(C_7H_6N_2) \cdot 4H_2O$: C, 45.12; N, 15.03; Cl, 15.22; H, 4.11%.

Physical measurements

Reflectance spectra of diluted compound in Li_2CO_3 were measured in the range 200–700 nm on a Hitachi spectrophotometer model 356 and undiluted samples were recorded on a Beckman UV 5240 spectrophotometer in the range 350–1000 nm. The EPR spectra at room temperature and 77 K were recorded on a JEOL-ME-3X spectrometer using a nuclear magnetometer MJ 110R and microwave frequency meter JES-SH-30X and a solid sample of Mn(II) in MgO as the reference. The EPR spectrum at liquid helium temperature was measured with an X-band Radiopan SE/X 2543 spectrometer. A solid sample of DPPH was used as the reference and the magnetic field was calibrated with proton and lithium NMR probes. The magnetic susceptibility of a polycrystalline sample of $[Cu_2Cl_3(C_7H_6N_2)_5]Cl \cdot 4H_2O$ was measured by the Faraday method over the temperature range 4.2–294 K, using a sensitive Cahn RG-HV electrobalance. The applied magnetic field was 6.2 kOe. The calibrant employed was $Hg[Co(NCS)_4]$, for which the magnetic susceptibility was taken to be 16.44×10^{-6} cm^3 g^{-1} [13]. The correction for diamagnetism of the constituent atoms was calculated by the use of Pascal's constants [14] and found to be -5.42×10^{-6} cm^3 mol^{-1}. The value 60×10^{-6} cm^3 mol^{-1} was used for the temperature-independent paramagnetism of copper(II) ion. Magnetism of the sample was found to be field independent. The effective magnetic moment was calculated from the equation $\mu_{eff} = 2.83(\chi_{Cu}T)^{1/2}$ BM.

X-ray data collection

The crystal used for data collection was a needle of approximate dimensions 0.2×0.3 mm cut to a length of 0.42 mm and mounted on an Enraf-Nonius CAD-4 diffractometer. The intensity data were collected using graphite-monochromated Mo Kα radiation and the ω–2θ scan mode, up to $\sin\theta/\lambda = 0.60$ Å^{-1}; 2.138 independent reflections with $I \geqslant 3\sigma(I)$ were used for the structure determination. Accurate cell parameters and the orientation matrix were refined by a least-square fit of the angular settings for 25 high-order reflections. The scan speed depended upon the intensity (from 1 to 6° min^{-1}). After every 75 reflections three standard reflections were measured to check misorientation and radiation damage. No radiation damage was observed. The intensity data were empirically corrected for absorption, using ψ scans around the diffraction vector of 8 selected reflections. The observed transmission varied from 57.9 to 76.1.

Crystal data

$C_{35}H_{38}N_{10}O_4Cl_4Cu_2$, $M_r = 931.6$, orthorhombic, $a = 19.506(3)$, $b = 17.384(4)$, $c = 11.940(2)$ Å, $V = 4048.8$ Å^3, $F(000) = 1904.0$, $Z = 4$, $D_c = 1.528$ M gm^{-3}, λ(Mo Kα) = 0.71069 Å, μ(Mo Kα) = 13.69 cm^{-1}, space group *Pnma*.

Structure determination

The structure was solved by direct methods. Positional and anisotropic thermal parameters for all non-hydrogen atoms were refined by full-matrix least-squares technique. The hydrogen atoms of benzimidazole ligands were located from geometrical considerations and these of water molecules from the difference Fourier map. The hydrogen atoms parameters were not refined (U(H) = 0.05 Å^2). The function $(|F_o| - |F_c|)^2$ was minimized, and in the final cycles of calculations a weighting scheme, based on counting statistics was used with $w = [\sigma^2(F_o) + 0.0045F_o^2]^{-1}$. After several cycles all shift/e.s.d. ratios were less than 0.1 and the refinement converged to agreement factors $R = 0.047$ and $R_w = 0.049$. The final difference Fourier map showed residual peaks from 0.8 to 0.4 Å^{-3} located on the symmetry plane near the middle of Cu–Cl, Cu–N, C–C and C–N bonds. Form factors were taken from the International Tables for X-Ray Crystallography [15]. Calculations were performed by the SHELX-76 and SHELXS-86 program packages [16], using an AMSTRAD 1512 microcomputer. Final atomic parameters are given in Tables 1, 2 and 3. See also 'Supplementary material'.

TABLE 1. Final atomic parameters of the non-hydrogen atoms ($\times 10^5$) for Cu atoms and ($\times 10^4$) for Cl, O, C, N atoms with e.s.d.s in parentheses

	x/a	y/b	z/c
Cu(1)	26669(5)	25000	17101(8)
Cu(2)	11102(5)	25000	4565(8)
Cl(1)	1506(1)	2500	2381(2)
Cl(2)	2307(1)	2500	−404(2)
Cl(3)	3792(1)	2500	2337(2)
Cl(4)	−2568(1)	2500	5722(2)
O(1)	3349(3)	1256(2)	4240(4)
O(2)	2903(3)	3663(3)	7668(4)
N(1)	2681(2)	1365(2)	1667(4)
N(3)	2468(3)	143(3)	2045(4)
N(11)	1068(2)	1362(2)	2477(4)
N(13)	1237(2)	137(2)	43(4)
N(21)	303(3)	2500	−589(6)
N(23)	−787(3)	2500	−1181(6)
C(2)	2310(3)	885(3)	2271(5)
C(4)	3317(3)	−462(4)	707(7)
C(5)	3799(4)	−261(4)	−83(7)
C(6)	3944(4)	516(5)	−310(6)
C(7)	3603(3)	1104(3)	214(5)
C(8)	3104(3)	914(3)	1003(5)
C(9)	2975(3)	136(3)	1240(5)
C(12)	1412(3)	873(3)	−166(5)
C(14)	387(3)	−453(3)	1391(6)
C(15)	−92(3)	−246(3)	2173(6)
C(16)	−203(3)	524(4)	2456(6)
C(17)	165(3)	1110(3)	1957(6)
C(18)	640(3)	913(3)	1145(5)
C(19)	746(3)	138(3)	865(5)
C(22)	−354(4)	2500	−303(7)
C(24)	−541(5)	2500	−3250(8)
C(25)	−3(5)	2500	−4017(7)
C(26)	670(5)	2500	−3639(8)
C(27)	844(4)	2500	−2509(9)
C(28)	298(4)	2500	−1762(7)
C(29)	−372(4)	2500	−2130(7)

TABLE 2. Final anisotropic thermal parameters ($\times 10^4$) for Cu atoms and ($\times 10^3$) for Cl, O, C, N atoms with e.s.d.s in parentheses[a]

	U_{11}	U_{22}	U_{33}	U_{23}	U_{13}	U_{12}
Cu(1)	326(5)	193(5)	461(6)	0	−50(5)	0
Cu(2)	333(5)	162(5)	495(6)	0	−62(5)	0
Cl(1)	40(1)	29(1)	43(1)	0	3(1)	0
Cl(2)	37(1)	28(1)	43(1)	0	2(1)	0
Cl(3)	36(1)	33(1)	64(1)	0	−14(1)	0
Cl(4)	47(1)	41(1)	88(2)	0	5(1)	0
O(1)	111(4)	36(2)	54(3)	4(2)	−3	24(2)
O(2)	125(4)	41(3)	64(3)	13(2)	−10(3)	0(3)
N(1)	36(2)	30(2)	42(3)	4(2)	0(2)	1(2)
N(3)	51(3)	22(2)	65(3)	4(2)	−2(3)	−4(2)
N(11)	31(2)	25(2)	49(3)	−1(2)	−4(2)	2(2)
N913)	52(3)	19(2)	53(3)	−8(2)	−3(3)	6(2)
N(21)	30(3)	19(3)	51(4)	0	−3(3)	0
N(23)	26(3)	32(3)	47(4)	0	−5(3)	0
C(2)	42(3)	30(3)	50(3)	6(3)	−3(3)	3(3)
C(4)	62(4)	32(4)	89(5)	−3(3)	−6(4)	11(3)
C(5)	75(5)	47(4)	86(5)	−22(4)	−5(5)	16(4)
C(6)	72(5)	66(5)	56(4)	−5(4)	−14(4)	8(4)
C(7)	51(3)	37(3)	53(4)	3(3)	−1(3)	3(3)
C(8)	35(3)	28(3)	45(3)	1(3)	−7(3)	3(2)
C(9)	44(3)	30(3)	54(4)	2(3)	−6(3)	1(2)
C(12)	38(3)	31(3)	45(3)	−3(3)	−1(3)	2(2)
C(14)	63(4)	27(3)	64(4)	2(3)	−11(3)	−6(3)
C(15)	54(4)	41(4)	65(4)	17(3)	1(4)	−15(3)
C(16)	45(3)	53(4)	61(4)	8(4)	11(3)	−4(3)
C(17)	41(3)	31(3)	65(4)	−5(3)	8(3)	6(3)
C(18)	37(3)	19(2)	48(3)	2(2)	−11(3)	0(2)
C(19)	42(3)	22(3)	47(3)	1(2)	−10(3)	3(2)
C(22)	37(5)	23(4)	54(5)	0	2(4)	0
C(24)	42(5)	47(5)	56(5)	0	−7(5)	0
C(25)	58(6)	74(7)	34(5)	0	−1(5)	0
C(26)	47(6)	72(7)	52(6)	0	7(5)	0
C(27)	31(4)	45(5)	72(7)	0	−4(5)	0
C(28)	42(5)	18(4)	49(5)	0	−6(4)	0
C(29)	28(4)	17(3)	61(6)	0	−14(4)	0

[a]Anisotropic temperature factor $T = \exp(2\Pi^2(U_{11}h^2a^{*2} + U_{22}k^2b^{*2} + U_{33}l^2c^{*2} + 2U_{12}hka^*b^* + 2U_{23}klb^*c^* + 2U_{13}hla^*c^*))$.

Results and discussion

A perspective view of the complex cation and the atom labelling scheme are presented in Fig. 1. Selected bond distances and angles are given in Table 4. The structure consists of binuclear cations $[Cu_2Cl_3(benzimidazole)_5]^+$, chloride anions and H_2O molecules. The complex cation of C_s symmetry is formed by two trigonal-bipyramidal copper(II) centers which share an edge by two equatorial chloride ligands. The equatorial coordination sites of Cu(1) atom are occupied by three chlorine ligands, while those of Cu(2) atom by two chloride and one benzimidazole ligand. The axial sites are occupied by the nitrogen atoms from four benzimidazole ligands. The Cu atoms and equatorial ligands are located on the symmetry plane. The Cu–Cu distance is 3.386(1) Å; the two shorter bridging Cu(1)–Cl(1) and Cu(2)–Cl(1) distances are 2.402(2) and 2.424(2) Å; the two longer Cu(1)–Cl(2) and Cu(2)–Cl(2) are 2.620(2) and 2.551(2) Å. The Cu(1)–Cl(1)–Cu(2) and Cu(1)–Cl(2)–Cu(2) angles are 89.1(1) and 81.8(1)°, respectively. The structure is the first example of a five-coordinated unsymmetrical copper(II) dinuclear complex with three equatorial and two axial Cu–L,X bonds where the Cu<X(1)X(2)>Cu bridge is formed by two unequivalent Cu–Cl–Cu bridges. One is formed by two short Cu–Cl bonds while the other by two long, semicoordinate Cu–Cl bonds. The literature data about the 4 + 1 coordination geometry for Cu(II) ions in binuclear complexes with three coplanar and

TABLE 3. Atomic coordinates of the hydrogen atoms ($\times 10^3$)

	x/a	y/b	z/c
H(2)	191	107	288
H(3)	224	−37	244
H(4)	321	−107	90
H(5)	408	−72	−53
H(6)	438	66	−95
H(7)	371	171	2
H(12)	179	105	−81
H(13)	145	−37	−37
H(14)	48	−105	118
H(15)	−38	−71	259
H(16)	−60	68	311
H(17)	9	171	220
H(22)	−48	250	65
H(23)	−137	250	−118
H(24)	−108	250	−352
H(25)	−12	250	−488
H(26)	112	250	−426
H(27)	139	250	−227
H(101)	339	154	354
H(102)	311	158	481
H(201)	269	346	827
H(202)	274	338	702

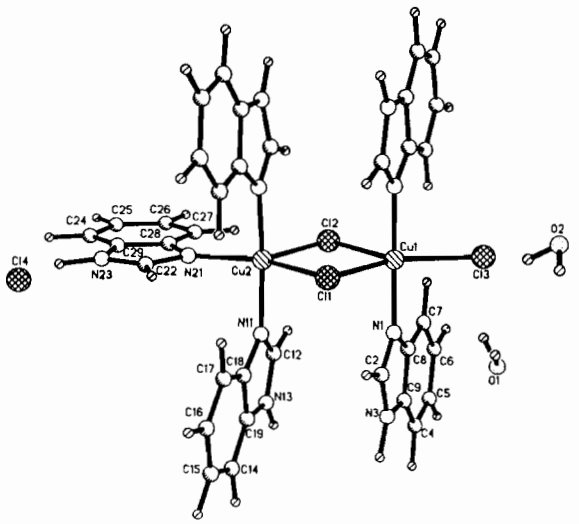

Fig. 1. A respective drawing of the $Cu_2Cl_3(C_7H_6N_2)_5$, Cl and H_2O molecules with the atom labelling scheme.

two axial ligands are reported in Table 5. The Cu(II) coordination polyhedron is described either as a deformed tetragonal pyramid or as a deformed trigonal bipyramid. In the present work the arrangement of the three ligands in the equatorial plane deviates from three-fold rotation axial symmetry, since only one of the three equatorial angles L,(X)–Cu–L,(X) is close to 120°. The three-fold rotation axial symmetry is deformed not only by the formation of a double bridge between the two copper atoms but also by the different lengths of the three equatorial bonds. One of them ($Cu–X_{b,\,sem}$) is always a semicoordinate bond with highly diversified lengths ($Cu–X_{b,\,sem}$ is from 2.447 to 3.075 Å). The angular bond arrangement observed here does not correspond to C_4 symmetry, as the four ligands with short Cu–L,(X) bonds do not lie in one plane (angles between *trans* bonds $L_{eq}–Cu–L_{eq}$ and $L_{ax}–Cu–L_{ax}$ deviate considerably from 180° and are in the range 134.0–152.9° and 161.8–176.7°).

The data in Table 5 indicate that two types of complexes are formed. Type I (with corresponding structures 1–4) is formed by sharing an edge joining two equatorial halogen atoms; type II by sharing an edge joining the axial and equatorial halogen ligands. The tetrahedron flattening angles are similar in both types of complexes (mean angle $L,(X)_{ax}–Cu–L_{ax}$ for types I and II is 172.8 and 169.9°, and mean of the largest $L,(X)_{eq}–Cu–L_{eq}$ angles is 144.2 and 143.1°, respectively). The sharing of the equatorial edge of the coordination polyhedron (type I) results in an increased diversification of the other two equatorial valency angles (mean values are 93.0 and 122.7° for type I and 98.7 and 117.7° for type II). The two types of complexes have a distinctly different geometry of the Cu  Cu bridge. In type I the values of Cu–X–Cu angles are always lower than 90°. For the three known $Cu\overset{sem}{\cdots}Cl–Cu$ bridges they are in the range 88.5–89.3°, while the angle $Cu\overset{sem}{\cdots}Br–Cu$ is 85.5°. For bridges $Cu\overset{sem}{\cdots}Cl\overset{sem}{\cdots}Cu$ and Cu–Cl–Cu found in the present work the angles are 81.8 and 89.1°, respectively. In type II this angle is always obtuse and as is shown by the data in Table 5 (structures 5–11) is close to 95° (from 92.1 to 97.9°). The average value of the distance Cu–Cu in the known structures of type I is smaller than that of type II and depends not so much upon the kind of halogen as upon the length of semicoordinate bonds $Cu\overset{sem}{\cdots}X$. Mean values of the Cu–Cu distance in complexes of type I and II are 3.569 and 3.740 Å, respectively. The Cu–Cu separation of 3.386(1) Å found in this work is the shortest Cu–Cu value in the considered binuclear complexes. In spite of the different values of analogous bond lengths, the data in Table 5 indicate a distinct elongation of Cu–X bonds by the formation of a bridge and non-equivalence of analogous axial and equatorial bonds. In a trigonal-bipyramidal model this last non-equivalence could result from minimization of electron pair repulsion, which is expected to lead to a shortening of the axial bond relative to the equatorial bonds for d^9 complexes [17]. In the investigated structure the differences between $Cu–N_{ax}$ and $Cu–N_{eq}$ lengths

TABLE 4. Bond lengths (Å) and angles (°)

Coordination sphere			
Cu(1)–Cl(1)	2.402(2)	Cu(2)–Cl(1)	2.424(2)
Cu(1)–Cl(2)	2.620(2)	Cu(2)–Cl(2)	2.551(2)
Cu(1)–Cl(3)	2.318(2)	Cu(2)–N(11)	1.980(4)
Cu(1)–N(1)	1.974(4)	Cu(2)–N(21)	2.010(4)
N(1)–Cu(1)–Cl(2)	88.8(1)	N(11)–Cu(2)–Cl(2)	92.5(1)
N(1)–Cu(1)–Cl(1)	91.2(1)	N(11)–Cu(2)–Cl(1)	90.1(1)
N(1)–Cu(1)–Cl(3)	89.7(1)	N(21)–Cu(2)–N(11)	88.6(1)
Cl(1)–Cu(1)–Cl(2)	93.9(1)	Cl(2)–Cu(2)–Cl(1)	95.2(1)
Cl(3)–Cu(1)–Cl(2)	124.4(1)	N(21)–Cu(2)–Cl(2)	117.8(1)
Cl(3)–Cu(1)–Cl(1)	141.7(1)	N(21)–Cu(2)–Cl(1)	147.0(1)
N(1)–Cu(1)–N(1′)	176.7(2)	N(11)–Cu(2)–N(11′)	175.0(2)
Cu(1)–Cl(1)–Cu(2)	89.1(1)	Cu(1)–Cl(2)–Cu(2)	81.8(1)
Benzimidazole ligands			
N(1)–C(2)	1.319(6)	N(1)–C(2)–N(3)	111.6(5)
C(2)–N(3)	1.354(7)	C(2)–N(3)–C(9)	108.2(5)
N(3)–C(9)	1.379(8)	N(3)–C(9)–C(8)	105.0(5)
C(9)–C(4)	1.391(9)	C(9)–C(8)–N(1)	108.8(5)
C(4)–C(5)	1.378(10)	C(8)–N(1)–C(2)	106.4(4)
C(5)–C(6)	1.408(10)	C(4)–C(5)–C(6)	120.9(6)
C(6)–C(7)	1.372(9)	C(5)–C(6)–C(7)	122.0(6)
C(7)–C(8)	1.395(8)	C(6)–C(7)–C(8)	118.1(6)
C(8)–N(1)	1.387(6)	C(7)–C(8)–C(9)	119.3(5)
C(8)–C(9)	1.406(8)	C(8)–C(9)–C(4)	122.9(6)
		C(9)–C(4)–C(5)	116.8(6)
N(11)–C(12)	1.329(6)	N(11)–C(12)–N(13)	111.8(5)
C(12)–N(13)	1.348(6)	C(12)–N(13)–C(19)	107.9(4)
N(13)–C(19)	1.372(7)	N(13)–C(19)–C(18)	106.0(4)
C(19)–C(14)	1.395(8)	C(19)–C(18)–N(11)	108.2(5)
C(14)–C(15)	1.371(9)	C(18)–N(11)–C(12)	106.0(4)
C(15)–C(16)	1.400(8)	C(14)–C(15)–C(16)	121.5(5)
C(16)–C(17)	1.383(8)	C(15)–C(16)–C(17)	121.4(6)
C(17)–C(18)	1.384(8)	C(16)–C(17)–C(18)	117.9(5)
C(18)–N(11)	1.394(6)	C(17)–C(18)–C(19)	120.2(5)
C(18)–C(19)	1.403(7)	C(18)–C(19)–C(14)	121.9(5)
		C(19)–C(14)–C(15)	117.1(5)
N(21)–C(22)	1.328(9)	N(21)–C(22)–N(23)	113.9(7)
C(22)–N(23)	1.345(10)	C(22)–N(23)–C(29)	105.6(6)
N(23)–C(29)	1.393(10)	N(23)–C(29)–C(28)	106.9(7)
C(29)–C(24)	1.377(12)	C(29)–C(28)–N(21)	109.0(7)
C(24)–C(25)	1.392(12)	C(28)–N(21)–C(22)	104.5(6)
C(25)–C(26)	1.391(13)	C(24)–C(25)–C(26)	119.9(8)
C(26)–C(27)	1.392(12)	C(25)–C(26)–C(27)	123.0(8)
C(27)–C(28)	1.390(12)	C(26)–C(27)–C(28)	115.8(8)
C(28)–N(21)	1.400(10)	C(27)–C(28)–C(29)	121.5(8)
C(28)–C(29)	1.380(10)	C(28)–C(29)–C(24)	122.4(8)
		C(29)–C(24)–C(25)	117.3(8)

are 0.029(6) and 0.035(6) Å, respectively, and support the trigonal-bipyramidal model of Cu(II) polyhedrons. The geometry of the benzimidazole ligands is similar as in other Cu(II) complexes [18]. Analogous bond lengths and angles of the three Cu-coordinated benzimidazole molecules show full agreement. The two benzimidazole molecules in the general position are roughly planar within ±0.016(7) Å. Figure 2 shows the molecular packing and the scheme of hydrogen bonds. The Cu atoms, equatorial ligands and Cl^- ions are located on the symmetry plane at 1/4 and 3/4b. The other benzimidazole molecules are almost perpendicular to the symmetry plane and pairwise parallel to each other (the angle between their best planes is 4.4(1)° and the angles with symmetry plane ar 89.25(9) and 93.53(9)°). The structure consists of consecutive layers containing Cu(II) ions and equatorial ligands and arranged in parallel

TABLE 5. Coordination geometry for Cu(II) ions in 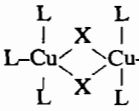 dimers with three coplanar (equatorial) and two axial Cu–X(L) bonds[a]

Coordination unit	Bond lengths (Å)[b]					Bond angles (°)[b]			Reference
	Cu–Cu	$Cu–X_{b/eq(ax)}$	$Cu–X_{b/eq/sem}$	$Cu–L_{ax}$	$Cu–L_{eq}$	$L,X_{eq}–Cu–L,X_{eq}$	$L_{ax}–Cu–L_{ax}$	Cu–X–Cu	
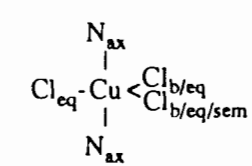	3.520	2.299	2.694	2.022 2.001	2.277	90.7 116.4 152.9	173.4	89.3	1
	3.448	2.441	2.544	1.989 1.980	2.260	92.5 129.0 138.5	176.5	87.5	
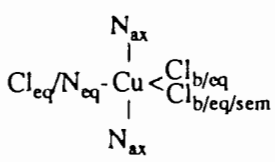	3.386	2.425	2.551	1.974	2.318(Cl)	95.2 117.8 147.0	175.0	89.1	this work
		2.402	2.620	1.980	2.009(N)	93.9 124.4 141.7	176.7	81.8	
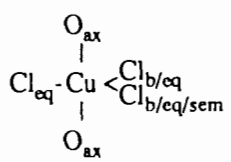	3.737	2.280	3.020	1.945 1.951	2.270	91.5 122.8 145.7	165.2	88.5	2
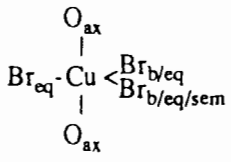	3.752	2.461	2.981	1.932 1.940	2.492	94.5 125.9 139.6	170.0	85.5	3
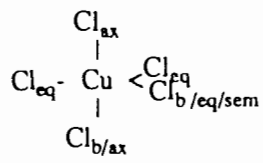	3.721	2.326	2.702	2.261	2.318 2.275	96.3 118.3 145.3	172.6	95.2	4

(continued)

TABLE 5. (*continued*)

Coordination unit	Bond lengths (Å)[b]					Bond angles (°)[b]			Reference
	Cu–Cu	$Cu–X_{b/eq(ax)}$	$Cu–X_{b/eq/sem}$	$Cu–L_{ax}$	$Cu–L_{eq}$	$L,X_{eq}–Cu–L,X_{eq}$	$L_{ax}–Cu–L_{ax}$	Cu–X–Cu	
Cl_{eq}-Cu(<Cl_{eq}, $Cl_{b/eq/sem}$)(Cl_{ax})($Cl_{b/ax}$)	3.700	2.318	2.705	2.253	2.320 2.290	96.2 117.2 146.6	173.9	94.6	5
	2.698	2.305	2.705	2.259	2.315 2.279	96.5 117.1 146.4	174.2	94.8	
N_{eq}-Cu(<Cl_{eq}, $Cl_{b/eq/sem}$)(Cl_{ax})($Cl_{b/ax}$)	3.572	2.288	2.447	3.326	2.366(Cl) 1.978(N)	111.7 114.3 134.0	168.7	97.9	6
N_{eq}-Cu(<Cl_{eq}, $Cl_{b/eq/sem}$)(N_{ax})($Cl_{b/ax}$)	3.805	2.464	2.796	1.953	2.265(Cl) 2.014(N)	89.0 121.0 149.7	171.1	96.9	7
Cl_{eq}-Cu(<S_{eq}, $Cl_{b/eq/sem}$)(S_{ax})($Cl_{b/ax}$)	3.749	2.266	2.825	2.308(S)	2.242(Cl) 2.369(S)	100.9 119.7 138.7	165.0	94.2	8
Cl_{eq}-Cu(<S_{eq}, $Cl_{b/eq/sem}$)(S_{ax})($Cl_{b/ax}$)	3.948	2.258	3.075	2.305(S) 2.230(Cl)	2.336(S)	99.5 113.3 146.1	161.8	94.3	9
	3.630	2.292	2.663	2.317(S) 2.255(Cl)	2.353(S)	103.4 116.6 139.6	168.6	93.9	
N_{eq}-Cu(<Br_{eq}, $Br_{b/eq/sem}$)(N_{ax})($Br_{b/ax}$)	3.803	2.468	2.802	2.310(Br) 2.018(N)	2.400(Br) 2.045(N)	95.0 122.2 141.6	172.8	92.1	10

[a]Symbols X = Cl, Br, L = Cl, Br, S, O, N; b = bridge, ax = axial, eq = equatorial, sem = semicoordinate. [b]The average e.s.d.s in the Cu–Cu, Cu–Br, Cu–Cl and Cu–S bonds lengths are 0.002 Å, in the Cu–O and Cu–N bond lengths are 0.006 Å, in the Cl–Cu–Cl, Br–Cu–Br and S–Cu–S bond angles are 0.1°, in the O–Cu–O and N–Cu–N angles are 0.3°.

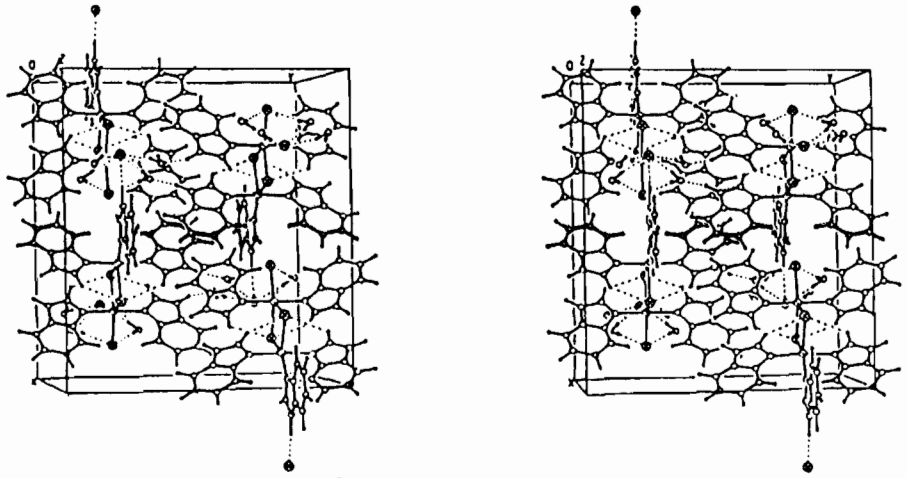

Fig. 2. The unit cell content of $[Cu_2Cl_3(C_7H_6N_2)_5]Cl \cdot 4H_2O$ showing hydrogen-bonding interactions.

benzimidazole ligands. The layers are joined by a network of hydrogen bonds through water molecules, each of them forming two O–H···Cl and one O···H–N bonds. Benzimidazole ligands also form two intermolecular hydrogen C–H···Cl bonds and an N–H···Cl bond lying in the symmetry plane. The geometry of the hydrogen bonds is presented in Table 6. A short van der Waals's contact (3.397(8) Å) is observed between C(2) and C(12) atoms of the two parallel benzimidazole rings of the complex cation.

The reflectance spectrum of the complex under investigation determined in the range 50–10 kK showed a few bands at 46.51, 40.00, 37.17, 36.23, 33.67 and 25.32 kK characteristic for the intra-ligand transitions of the benzimidazole molecule and ligand to metal charge-transfer transitions. Furthermore, the broad band at 13.89 kK is attributed to a d–d transition of copper(II) ion in the trigonal-bipyramidal ligand field [20].

The EPR powder spectra of the complex recorded in the X-band at room temperature and 77 K exhibit two components related to $g_\perp = 2.21$ and $g_\parallel = 2.02$ parameters. The observed EPR spectrum is the average spectrum of two copper centers in the ligand field of the distorted trigonal-bipyramidal symmetry $Cu(1)N_2Cl_3$ and $Cu(2)N_3Cl_2$, respectively. The exchange interaction between Cu(II) centers was confirmed only by the presence of the fragment superhyperfine structure in the low field part of the spectrum ($A = 48$ Oe). The EPR spectrum at 4.2 K indicated the same character as at the higher temperatures. Only lowering values of the spectroscopic splitting factors were observed ($g_\perp = 2.19$ and $g_\parallel = 2.00$).

Magnetic data for a powdered sample of the binuclear complex were collected over the temperature range 4.2–295 K. Plots of inverse magnetic susceptibility, χ_{Cu}^{-1}, and μ_{eff} as a function of temperature are shown in Fig. 3. The data revealed a linear course of the $\chi_{Cu}^{-1} = f(T)$ relation, although the different C and θ constants observed for temperature ranges 4.2–25 K ($C = 0.484$ cm^3 mol^{-1} K, $\theta = -1.1$ K, $R = 5.92 \times 10^{-4}$) and 50–295 K ($C = 0.446$ cm^3 mol^{-1} K, $\theta = 0.1$ K, $R = 5.16 \times 10^{-8}$), respectively [$R = \Sigma(\chi_i^{exp} - \chi_i^{calc})^2$]. On cooling the system the μ_{eff} exhibits an increase from 1.886 BM at 295 K, and reaches a maximum of 1.919 BM at 15 K. Such an increase could be combined with an intramolecular ferromagnetic interaction. Further temperature lowering results in a decrease of μ_{eff} to 1.758 BM at 4.2 K, characteristic of a weak antiferromagnetic interaction between the binuclear units within the crystal lattice, superimposed on the ferromagnetic intramolecular coupling. The energy separation, $2J$, between the ground triplet and excited singlet states can be derived from the following equation for the magnetic susceptibility for two exchange coupled copper(II) ions [21], with a molecular field correction [22, 23]

$$\chi_{Cu}^{corr} = \chi_{Cu}/[1 - (2zJ'\chi_{Cu}/N\beta^2g^2)]$$

$$\chi_{Cu} = (N\beta^2g^2/3KT)\left[1 + \frac{1}{3}\exp(2J/KT)\right]^{-1}$$

where all the symbols have their usual meaning. The observed experimental magnetic susceptibility data were fitted by the least-squares method to the above model and the best fit values obtained were $2J = 5.6$ cm^{-1}, $J' = -0.6$ cm^{-1} (for $z = 4$) and agreement factor $R = 1.25 \times 10^{-5}$. The spectroscopic splitting factor $\langle g \rangle = 2.15$ (obtained from the EPR spectrum) was used in the fitting process as a constant.

A further insight concerning the electronic structure, as well as the exchange mechanism of the

TABLE 6. Hydrogen bonds (Å) and angles (°)[a]

D–H	D··A[b]	H··A[b]	D–H··A[b]
C(2)–H(2) 1.112(6) 1.080	C(2)··Cl(1) 3.219(5)	H(2)··Cl(1) 2.669(1) 2.680	C(2)–H(2)··Cl(1) 109.7(3) 110.3
C(12)–H(2) 1.116(6) 1.080	C(12)··Cl(2) 3.336(6)	H(12)··Cl(2) 2.761(1) 2.761	C(12)–H(12)··Cl(2) 112.4(3) 113.1
O(1)–H(101) 0.982(4) 0.938	O(1)··Cl(3) 3.254(5)	H(101)··Cl(3) 2.328(2) 2.368	O(1)–H(101)··Cl(3) 156.9(3) 157.3
O(1)–H(102) 0.999(5) 0.938	O(1)··Cl(4) 3.183(5)	H(102)··Cl(4) 2.206(2) 2.265	O(1)–H(102)··Cl(4) 165.4(2) 165.8
O(2)–H(202) 0.972(5) 0.938	O(2)··Cl(4) 3.149(5)	H(202)··Cl(4) 2.205(2) 2.237	O(2)–H(202)··Cl(4) 163.5(2) 163.7
O(2)–H(201) 0.909(5) 0.938	O(2)··Cl(2)^{I} 3.277(5)	H(201)··Cl(2)^{I} 2.412(2) 2.385	O(2)–H(201)··Cl(2)^{I} 159.0(2) 159.0
N(3)–H(3) 1.103(5) 1.030	N(3)··O(2)^{II} 2.774(6)	H(3)··O(2)^{II} 1.728(4) 1.795	N(3)–H(3)··O(2)^{II} 156.5(3) 157.5
N(13)–H(13) 1.087(4) 1.030	N(13)··O(1)^{III} 2.727(5)	H(13)··O(1)^{III} 1.662(4) 1.717	N(13)–H(13)··O(1)^{III} 165.3(3) 165.8
N(23)–H(23) 1.135(6) 1.030	N(23)··Cl(4)^{IV} 3.253(6)	H(23)··Cl(4)^{IV} 2.143(3) 2.245	N(23)–H(23)··Cl(4)^{IV} 165.2(4) 165.9

[a]Values normalized following ref. 19. [b]Equivalent positions: (I) $x, y, z+1$; (II) $-x+0.5, y-0.5, z-0.5$; (III) $-x+0.5, -y, z-0.5$; (IV) $x-0.5, -y+0.5, -z+0.5$.

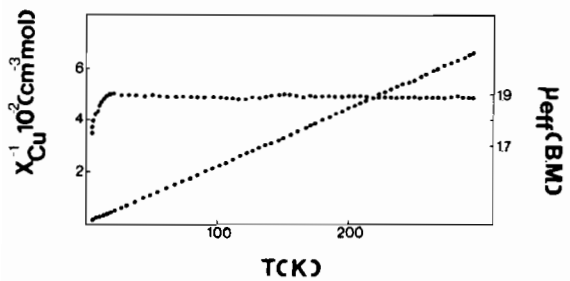

Fig. 3. Experimental magnetic data plotted as μ_{eff} and inverse magnetic susceptibility, χ_{Cu}^{-1} vs. temperature for $[Cu_2Cl_3(C_7H_6N_2)_5]Cl \cdot 4H_2O$.

complex under investigation, was also gained through Extended Hückel Molecular Orbital Calculations (EHMO). These calculations were carried out on the actual geometry of the complex, obtained from the solved X-ray structure, with parametrization published elsewhere [24, 25]. Furthermore, to limit the calculation time and the basis set, the benzimidazole ligands were substituted by the model molecular fragment $[HN=CH_2]$, with the copper–nitrogen bond lengths being those found in the actual structure.

The net charges calculated for the atoms of main interest, as well as the overlap populations for all the coordination bonds, are depicted schematically in Fig. 4. Despite the quite different environment of each copper atom the net charges calculated were almost identical. This is also true for the two bridging chlorine atoms. These facts along with the small negative values of the other bonded atoms support the idea of an extended covalency of all the metal–ligand bonds in the complex. Of particular interest are the overlap populations calculated for the bonds in the Cu 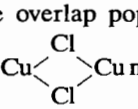 Cu moiety. Thus the negative repulsive Cu–Cu overlap population calculated (−0.057) excludes any bonding interaction between the two metallic centers. Furthermore the four bridging Cu–Cl bonds are apart from been symmetric. The bonds between the copper atoms and the one bridging chlorine, Cl(1), are stronger than the cor-

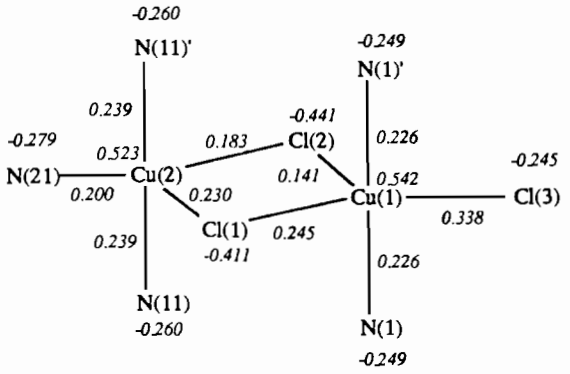

Fig. 4. EHMO net charges and overlap populations of selected atoms and bonds calculated for the complex under investigation (labelling scheme as in Fig. 1).

responding bonds for the second bridging atom, Cl(2). Thus, due to the quite small overlap population values of the latter bonds, semicoordination is a better suggestion for them, in close agreement with the crystallographic data of the complex.

The mechanism of the magnetic coupling present in the complex was also investigated on the basis of the orbital model developed by Hoffmann and co-workers [25]. The most possible pathway existing in this complex is the intramolecular one, because of the absence of intermolecular distances between the copper atoms indicative for an intermolecular interaction. The two single occupied molecular orbitals (SOMOs), obtained by the EHMO calculations are shown in Fig. 5. In these SOMOs, located mainly on each d_{z^2} atomic orbital of the copper centers, there is a partial delocalization of the spin density on the two bridging chlorine atoms and the other atoms ligated to each center. Such a localization of the spin density on the coordination sphere of the one magnetic center only is due to the low symmetry of the molecule and accounts well for the observed ferromagnetic interaction.

Hodgson and co-workers [12] have shown that for bis-chloro-bridged Cu(II) binuclear complexes, wherein the copper centers adopt square-pyramidal or trigonal-bipyramidal geometry, an empirical correlation exists between the exchange energy $2J$ and the φ/R ratio, where φ is the Cu–Cl–Cu bridging angle and R the longer Cu–Cl distance within the bridge. Due to existence of the two non-equivalent Cu–Cl–Cu bridges in the present complex one can calculate a mean φ/R ratio equal to 33.9. For this φ/R value the empirical correlation predicts weak ferromagnetic exchange for this complex with an exchange energy, $2J$, of few cm^{-1} in agreement with the observed ferromagnetic interaction.

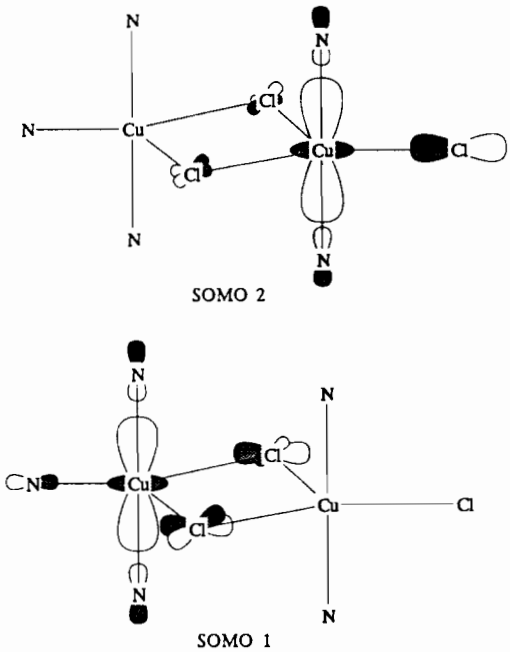

Fig. 5. The two SOMOs of the complex under investigation.

Supplementary material

Tables of observed and calculated structure factors are available from the authors.

References

1 I. Sotofte and K. Nielsen, *Acta Chem. Scand., Ser. A, 35* (1981) 733.
2 D. D. Swank, G. F. Needham and R. D. Willett, *Inorg. Chem., 18* (1979) 761.
3 C. P. Landee and R. E. Greeney, *Inorg. Chem., 25* (1986) 3772.
4 D. J. Hodgson, P. K. Hale and W. E. Hatfield, *Inorg. Chem., 10* (1971) 1061.
5 S. K. Hoffmann, D. J. Hodgson and W. E. Hatfield, *Inorg. Chem., 24* (1985) 1194.
6 J. P. Declercq, M. Debbaudt and M. van Meerssche, *Bull. Soc. Chim. Belg., 80* (1971) 527.
7 I. P. Lavrent'ev, L. G. Korableva, E. A. Lavrent'eva, G. A. Nifontova, M. L. Khidekel, I. G. Gusakovsksys, T. I. Larkina, L. D. Arutyunyan, O. S. Filipenko, V. I. Ponomarev and L. O. Atovmyan, *Transition Met. Chem., 5* (1980) 193.
8 B. Cohen, C. C. Ou, R. A. Lalancétte, W. Borowski, J. A. Potenza and H. J. Schugar, *Inorg. Chem., 18* (1979) 217.
9 W. E. Hatfield, L. W. Haar, M. M. Olmstead and W. K. Musker, *Inorg. Chem., 25* (1986) 558.
10 R. B. Wilson, W. E. Hatfield and D. J. Hodgson, *Inorg. Chem., 15* (1976) 1712.
11 E. Kwiatkowski, M. Kwiatkowski, A. Olechnowicz, J. Mrozinski, D. M. Ho and E. Deutsch, *Inorg. Chim. Acta, 158* (1989) 37.

12 W. E. Marsh, K. C. Patel, W. E. Hatfield and D. J. Hodgson, *Inorg. Chem., 22* (1983) 511.
13 B. N. Figgis and R. S. Nyholm, *J. Chem. Soc.,* (1958) 4190.
14 E. Köning, *Magnetic Properties of Coordination and Organometallic Transition Metal Compounds,* Springer, Berlin, 1966.
15 *International Tables for X-ray Crystallography,* 1974.
16 *SHELX-76* and *SHELXS-86.*
17 R. J. Gillespie, *J. Chem. Soc.,* (1963) 4679.
18 M. Bukowska-Strzyzewska and A. Tosik, *J. Crystallogr. Spectrosc. Res., 18* (1988) 713.
19 G. A. Jeffrey and L. Lewis, *Carbohydr. Res., 60* (1978) 179; R. Taylor and O. Kennard, *Acta Crystallogr., Sect. B, 39* (1983) 133.
20 W. D. Harrisson, D. M. Kennedy, M. Power, R. Sheahan and B. J. Hathaway, *J. Chem. Soc., Dalton Trans.,* (1981) 1463.
21 B. Bleaney and K. D. Bowers, *Proc. R. Soc. London, Ser. A, 214* (1952) 451.
22 J. W. Stout and R. C. Chisholm, *J. Chem. Phys., 36* (1962) 979.
23 D. K. Towle, S. K. Hoffmann, W. E. Hatfield, P. Singh, P. Caudhuri and K. Weighardt, *Inorg. Chem., 24* (1985) 4393.
24 G. J. Burns, *Chem. Phys., 41* (1964) 1521.
25 P. J. Hay, J. C. Thibeault and R. J. Hoffmann, *J. Am. Chem. Soc., 97* (1975) 4884.